J. Radiat. Res., 52, 680–684 (2011)

Technical Report

T2*-weighted Image/T2-weighted Image Fusion in Postimplant Dosimetry of Prostate Brachytherapy

Norihisa KATAYAMA[1*], Mitsuhiro TAKEMOTO[2], Kotaro YOSHIO[2], Kuniaki KATSUI[2], Tatsuya UESUGI[3], Yasutomo NASU[3], Toshi MATSUSHITA[4], Mitsumasa KAJI[4], Hiromi KUMON[3] and Susumu KANAZAWA[2]

Prostate cancer/Brachytherapy/Postimplant dosimetry/MRI/T2*-weighted image.

Computed tomography (CT)/magnetic resonance imaging (MRI) fusion is considered to be the best method for postimplant dosimetry of permanent prostate brachytherapy; however, it is inconvenient and costly. In T2*-weighted image (T2*-WI), seeds can be easily detected without the use of an intravenous contrast material. We present a novel method for postimplant dosimetry using T2*-WI/T2-weighted image (T2-WI) fusion. We compared the outcomes of T2*-WI/T2-WI fusion-based and CT/T2-WI fusion-based postimplant dosimetry. Between April 2008 and July 2009, 50 consecutive prostate cancer patients underwent brachytherapy. All the patients were treated with 144 Gy of brachytherapy alone. Dose-volume histogram (DVH) parameters (prostate D90, prostate V100, prostate V150, urethral D10, and rectal D2cc) were prospectively compared between T2*-WI/T2-WI fusion-based and CT/T2-WI fusion-based dosimetry. All the DVH parameters estimated by T2*-WI/T2-WI fusion-based dosimetry strongly correlated to those estimated by CT/T2-WI fusion-based dosimetry ($0.77 \leq R \leq 0.91$). No significant difference was observed in these parameters between the two methods, except for prostate V150 ($p = 0.04$). These results show that T2*-WI/T2-WI fusion-based dosimetry is comparable or superior to MRI-based dosimetry as previously reported, because no intravenous contrast material is required. For some patients, rather large differences were observed in the value between the 2 methods. We thought these large differences were a result of seed miscounts in T2*-WI and shifts in fusion. Improving the image quality of T2*-WI and the image acquisition speed of T2*-WI and T2-WI may decrease seed miscounts and fusion shifts. Therefore, in the future, T2*-WI/T2-WI fusion may be more useful for postimplant dosimetry of prostate brachytherapy.

INTRODUCTION

Permanent prostate brachytherapy with ^{125}I or ^{103}Pd has become a standard treatment option for patients with localized prostate cancer.[1,2)]

Postimplant dosimetry is a standard tool for assessing implant quality. According to the recommendations of the American Brachytherapy Society (ABS) and the European Society for Therapeutic Radiology and Oncology/European Association of Urology/European Organization for Research and Treatment of Cancer (ESTRO/EAU/EORTC), postimplant dosimetric analysis should be performed for all patients undergoing permanent prostate brachytherapy.[3,4)] It has been shown in postimplant dosimetry, that the probability of achieving biochemical control is related to the prostate dose[5,6)] and that the probability of inducing complications is related to the urethral and rectal doses.[7,8)] Therefore, it is important to accurately know the doses absorbed by the target volume and the organs at risk. Postimplant dosimetry plays a very important role in the assessment of these parameters.

Computed tomography (CT)/magnetic resonance imaging (MRI) fusion is regarded as the best method for postimplant dosimetry.[9–11)] However, using both CT and MRI for postimplant dosimetry is inconvenient and costly.[10)] To date, only 1 study has used MRI-based postimplant dosimetry in a large number of patients;[10)] however, a considerable number of extraprostatic seeds were not successfully counted in MRI scans, and an intravenous contrast material was used.

In T2*-weighted image (T2*-WI), metallic implants, such

*Corresponding author: Phone: +81-79-294-2251,
Fax: +81-79-296-4050,
E-mail: n-katayama@bea.hi-ho.ne.jp
[1]Department of Radiology, Japanese Red Cross Society Himeji Hospital, 1-12-1 Shimoteno, Himeji 670-8540, Japan; [2]Department of Radiology, Okayama University Hospital, 2-5-1 Shikata-cho, Kita-ku, Okayama 700-8558, Japan; [3]Department of Urology, Okayama University Hospital, 2-5-1 Shikata-cho, Kita-ku, Okayama 700-8558, Japan; [4]Okayama Diagnostic Imaging Center, 2-3-25 Daiku, Kita-ku, Okayama 700-0913, Japan.
doi:10.1269/jrr.11011

as seeds, result in loss of signal intensity and produce signal intensity artifacts.[12] Therefore, seed detection is facilitated in the absence of an intravenous contrast material. Because the prostate and urethra are poorly defined in T2*-WI, we hypothesized that results obtained by T2*-WI/T2-weighted image (T2-WI) fusion are as accurate as those obtained by CT/MRI fusion. Therefore, to estimate the accuracy of T2*-WI/T2-WI fusion-based dosimetry, we compared the results obtained from T2*-WI/T2-WI fusion-based and CT/T2-WI fusion-based dosimetry.

MATERIALS AND METHODS

Between April 2008 and July 2009, 50 consecutive patients with low-risk or intermediate-risk prostate cancer (prostate specific antigen level, ≤ 20 ng/ml; Gleason score, 6–7; Union Internationale Contre le Cancer 2002 clinical stage, T1–T2) were treated with brachytherapy at Okayama University Hospital. All patients were treated with 144 Gy of brachytherapy alone.

All the patients were treated using loose ^{125}I radioactive seeds (Oncoseed; Nihon Mediphysics Co., Tokyo, Japan) loaded with a Mick applicator (Mick Radio-Nuclear Instruments Inc., Bronx, New York, USA). The Variseed ver. 8.0.1 (Varian Medical Systems Inc., Palo Alto, California, USA) software was used for both planning and calculating the final dosimetry.

The 0.35 mCi ^{125}I seeds were peripherally loaded using real-time ultrasound-guided seed placement and intraoperative dosimetry. Dose–volume constraints were as follows: the prostate V100, the percentage of the prostate gland that receives 100% of the prescribed dose, > 98%; urethral D1, the dose irradiating 1% of the urethral volume, < 220 Gy; and rectal D1, the dose irradiating 1% of the rectal volume, < 144 Gy. The mean number of seeds was 78.6 (range, 58–98). The mean volume of the postimplant prostate was 26.22 cc (range, 15.24–38.23 cc).

The American Association of Physicists in Medicine (AAPM) Task Group 43 (TG-43) formula was used for calculating the final dosimetry.[13] Point dose calculation was used.

Postimplant image acquisition techniques

Thirty days after implant, a chest radiograph (anteroposterior view), kidney-urinary bladder (KUB) radiograph, and pelvic radiograph were taken to check for any possible seed migration. On the same day, pelvic CT and MRI were performed at Okayama Diagnostic Imaging Center to evaluate the dosimetry. No urinary catheter was put in place.

A postimplant CT scan was performed using a CT scanner with 64 detector arrays (Aquilion 64; Toshiba Medical Systems Co., Tokyo, Japan). Axial CT images in 1-mm thickness with 1-mm intervals were obtained. For these scans, a field of view (FOV) of 16 cm, a 512-square matrix, and a standard reconstruction algorithm were used (Fig. 1a).

Within 1 h after the CT, a postimplant MRI scan was performed using a magnetic resonance (MR) imager (Magnetom Avanto 1.5T; Siemens AG, Erlangen, Germany). We obtained 2 sequences of T2-WI and T2*-WI using a 6-channel body matrix coil and a 6-channel spine matrix coil. Technical parameters of T2-WI were as follows: repetition time (TR)/echo time (TE) in milliseconds, 3950/83; FOV, 14 cm; slice thickness, 3 mm without a gap; matrix size, 205 × 256; band width, 130 Hz/pixel; echo train length, 9; flip angle, 180 degree; average, 4; parallel imaging, generalized autocalibrating partially parallel acquisition (GRAPPA)-2; over sampling, 40%; scan time, 257 s (Fig. 1b). T2*-WI was obtained through a multi-echo gradient sequence, and technical parameters were as follows: TR/TE, 563/14; FOV, 14 cm; slice thickness, 3 mm without a gap; matrix size, 205 × 256; band width, 220 Hz/pixel; combined echos, 3; flip angle, 30 degree; average, 3; parallel imaging, GRAPPA-2; over sampling, 40%; scan time, 262 s (Fig. 1c). T2-WI and T2*-WI were obtained successively. In T2-WI, the prostate was well defined, but it was difficult to visualize the seeds. Conversely, in T2*-WI, it was easy to visualize the seeds, but the prostate was poorly defined. We were able to visualize the urethra in T2-WI.

No intravenous contrast material was used in the CT or MRI scans.

CT/T2-WI fusion-based dosimetry

In CT, the seeds were detected automatically by using the Variseed system, and the rectum was manually contoured because the rectum was well defined also in the CT in which the seeds were detected. In T2-WI, the prostate and urethra were manually contoured.

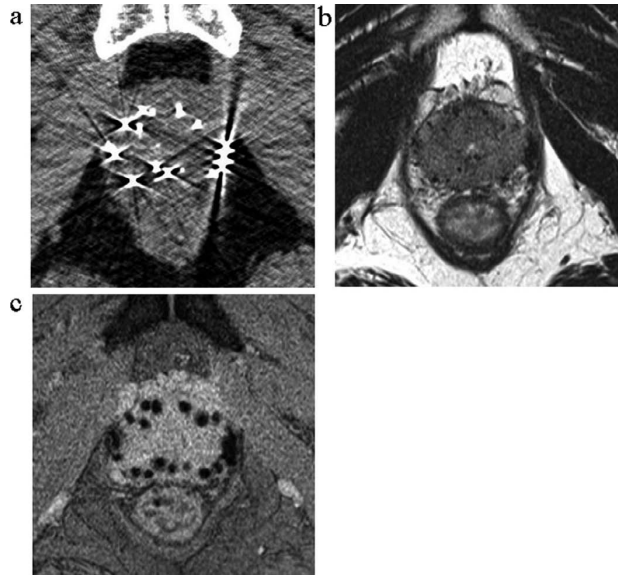

Fig. 1. Corresponding axial-slice images of the postimplant prostate. (a) CT, (b) T2-WI, (c) T2*-WI. CT, computed tomography; T2-WI, T2-weighted image; T2*-WI, T2*-weighted image.

The CT and T2-WI were electronically fused using the manual-fusion procedure of the Variseed fusion system. We identified 6 or more corresponding seed pairs in the CT and T2-WI and then used the Variseed program to calculate the transformation. This fusion procedure was performed until the positions of the seeds in the CT corresponded with those in the T2-WI.

T2-WI/T2-WI fusion-based dosimetry*

The T2-WI images in which the prostate and urethra had been contoured for the CT/T2-WI fusion-based dosimetry were imported and used for T2*-WI/T2-WI fusion-based dosimetry. In T2*-WI, the seeds were detected, and the rectum was manually contoured because the rectum was well defined also in the T2*-WI in which the seeds were detected. The seeds were initially identified on each slice and later sorted using the VariSeed redundancy-correction module to reduce the number of seeds to the number implanted. If the positions of the seeds in the T2*-WI did not correspond with those in the T2-WI, a fusion procedure similar to CT/T2-WI fusion was performed.

Comparison of T2-WI/T2-WI fusion-based and CT/T2-WI fusion-based dosimetry*

The same radiation oncologist (N.K.) performed T2*-WI/T2-WI fusion-based and CT/T2-WI fusion-based dosimetry for all patients, and the results were confirmed by a second radiation oncologist (M.T.). Both were well trained in post-implant dosimetry of permanent prostate brachytherapy. T2*-WI/T2-WI fusion-based dosimetry was performed more than 1 month after CT/T2-WI fusion-based dosimetry in order to avoid bias in the measurements.

T2*-WI/T2-WI fusion-based dosimetry and CT/T2-WI fusion-based dosimetry were compared on the basis of dose–volume histogram (DVH) parameters (prostate D90, dose irradiating 90% of the prostate volume; prostate V100, percentage of the prostate gland that receives 100% of the prescribed dose; V150, percentage of the prostate gland that receives 150% of the prescribed dose; urethral D10, dose irradiating 10% of the urethral volume; and rectal D2 cc, dose irradiating 2 cc of the rectum), as recommended by the ESTRO/EAU/EORTC. The DVH parameters were compared between T2*-WI/T2-WI fusion-based and CT/T2-WI fusion-based dosimetry using a paired *t* test, and the correlations between the DVH parameter values obtained in each procedure were estimated using Pearson's correlation coefficient.

The detection accuracy of all seeds and extraprostatic seeds on T2*-WI compared to CT was checked.

Data processing and statistical analyses were carried out using SPSS 11.0 (SPSS, Chicago, IL).

Comparison of CT-based and CT/T2-WI fusion-based dosimetry

This comparison was performed in a similar manner to the comparison of T2*-WI/T2-WI fusion-based and CT/T2-WI fusion-based dosimetry.

RESULTS

It took approximately 10 min to fuse CT and T2-WI. In 49 patients, the positions of the seeds in the T2*-WI corresponded with those in the T2-WI; therefore, it took little time to fuse T2*-WI and T2-WI. In 1 patient, the positions of the seeds in the T2*-WI did not correspond with those in the T2-WI; therefore, the abovementioned fusion procedure was performed. The seeds were detected in the T2*-WI in approximately 10 min. The approximate time required for T2*-WI/T2-WI fusion-based dosimetry and CT/T2-WI fusion-based dosimetry was 20 to 30 min each.

The values of the DVH parameters were compared between T2*-WI/T2-WI fusion-based and CT/T2-WI fusion-based dosimetry (Table 1, Fig. 2 and 3). No significant differences were observed between the procedures with regard to the prostate D90, prostate V100, urethral D10, or rectal D2cc values. The prostate V150 value estimated by T2*-WI/T2-WI fusion-based dosimetry was significantly lower than that estimated by CT/T2-WI fusion-based dosimetry. The values of all the DVH parameters estimated by T2*-WI/T2-WI fusion-based dosimetry strongly correlated to those estimated by CT/T2-WI fusion-based dosimetry.

A comparison of DVH parameters between CT-based and CT/T2-WI fusion-based dosimetry is shown in Table 2.

The detection accuracy of all seeds and extraprostatic seeds by using T2*-WI was 93.2% ± 2.3% (mean ± standard

Table 1. Comparison of DVH parameters between T2*-WI/T2-WI fusion-based and CT/T2-WI fusion-based dosimetry (mean ± standard deviation)

DVH Parameters	T2*/T2	CT/T2	95% CI (Paired *t* test)	*p* (Paired *t* test)	R	95% CI (Correlation)	*p* (Correlation)
Prostate D90 (Gy)	170.66 ± 17.54	171.62 ± 19.19	–1.87–3.78	0.50	0.86	0.76–0.92	< 0.001
Prostate V100 (%)	95.50 ± 3.48	95.59 ± 3.55	–0.44–0.63	0.72	0.86	0.76–0.92	< 0.001
Prostate V150 (%)	66.45 ± 13.10	68.10 ± 13.19	0.08–3.19	0.04	0.91	0.85–0.95	< 0.001
Urethral D10 (Gy)	242.91 ± 29.74	245.73 ± 33.21	–2.46–8.10	0.29	0.83	0.72–0.90	< 0.001
Rectal D2cc (Gy)	98.85 ± 16.25	96.34 ± 16.83	–5.70–0.67	0.12	0.77	0.63–0.86	< 0.001

Abbreviations: DVH, dose–volume histogram; T2*-WI, T2*-weighted image; T2-WI, T2-weighted image; T2*/T2, T2*-WI/T2-WI fusion-based dosimetry; CT, computed tomography; CT/T2, CT/T2-WI fusion-based dosimetry; CI, confidence interval

Table 2. Comparison of DVH parameters between CT-based and CT/T2-WI fusion-based dosimetry (mean ± standard deviation)

DVH Parameters	CT	CT/T2	95% CI (Paired *t* test)	*p* (Paired *t* test)	R	95% CI (Correlation)	*p* (Correlation)
Prostate D90 (Gy)	159.89 ± 20.33	171.62 ± 19.19	7.28–16.17	< 0.001	0.69	0.51–0.81	< 0.001
Prostate V100 (%)	93.15 ± 4.71	95.59 ± 3.55	1.38–3.51	< 0.001	0.62	0.42–0.77	< 0.001
Prostate V150 (%)	64.47 ± 12.71	68.10 ± 13.19	2.35–4.91	< 0.001	0.94	0.90–0.97	< 0.001
Urethral D10 (Gy)	252.48 ± 38.60	245.73 ± 33.21	–12.82—0.69	0.030	0.83	0.72–0.90	< 0.001
Rectal D2cc (Gy)	96.89 ± 17.45	96.34 ± 16.83	–1.32–0.23	0.16	0.99	0.98–0.99	< 0.001

Abbreviations: DVH, dose–volume histogram; CT, computed tomography; T2-WI, T2-weighted image; CT/T2, CT/T2-WI fusion-based dosimetry; CI, confidence interval

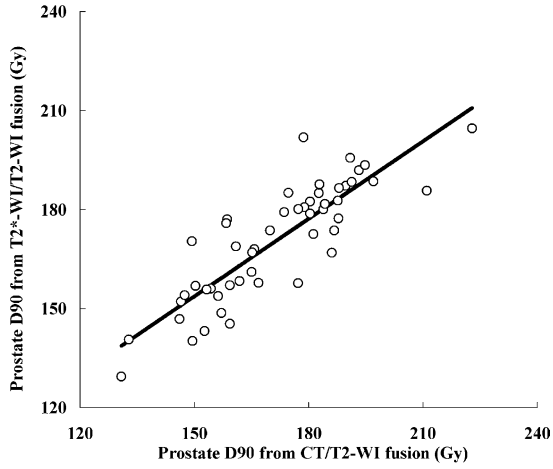

Fig. 2. Comparison of the prostate D90 between T2*-WI/T2-WI fusion-based and CT/T2-WI fusion-based dosimetry. T2*-WI, T2*-weighted image; T2-WI, T2-weighted image; CT, computed tomography.

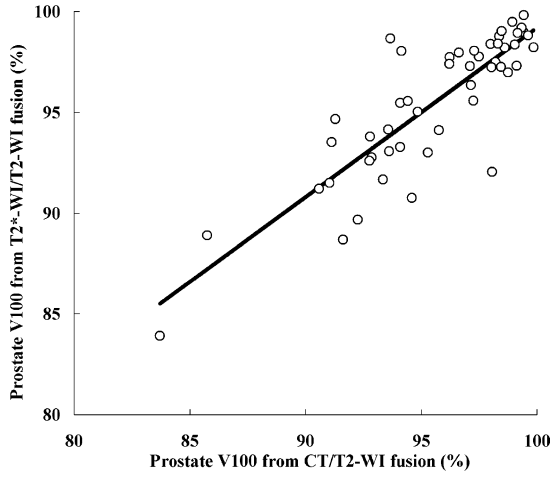

Fig. 3. Comparison of the prostate V100 between T2*-WI/T2-WI fusion-based and CT/T2-WI fusion-based dosimetry. T2*-WI, T2*-weighted image; T2-WI, T2-weighted image; CT, computed tomography.

deviation [SD]) and 93.3% ± 7.6%, respectively. Miscounts mainly occurred in the clusters of seeds. The number of clustered seeds was often underestimated in T2*-WI.

DISCUSSION

In CT, it is easy to visualize seeds, but anatomical structures are poorly defined.[14,15] Conversely, in T2-weighted MRI scans, anatomical structures are well defined, but it is difficult to visualize seeds.[16] Amdur *et al.* exploited the advantages of both of these modalities and fused CT and MRI scans with a high degree of accuracy.[17] Polo *et al.* observed significant differences in prostate volume between CT and CT/MRI fusion scans, but a strong correlation in DVH parameters was observed between the two procedures.[18] Tanaka *et al.* reported that prostate D90 and V100 values were significantly underestimated in CT-based dosimetry compared with CT/MRI fusion-based dosimetry.[19] In our results, significant differences were observed between CT-based and CT/T2-WI fusion-based dosimetry with regard to the prostate D90, V100, V150, and urethral D10 values. On the basis of the results of these studies, CT/MRI fusion is regarded to be the best method for postimplant dosimetry.[9,10] However, the use of both CT and MRI for postimplant dosimetry is inconvenient and costly.[10]

Only one study has been published about MRI-based postimplant dosimetry in a large number of patients.[10] The authors compared the DVH parameters between MRI-based and CT/MRI fusion-based dosimetry. The values of prostate D90, V100, V150, and V200 were all significantly overestimated in MRI-based dosimetry compared with CT/MRI fusion-based dosimetry because the mean success rate in locating the extraprostatic seeds using MRI was 78.4%. Furthermore, although contrast-enhanced T1-weighted image (CE-T1WI) were used for both MRI-based and CT/MRI fusion-based dosimetry, an intravenous contrast material is costly and invasive and cannot be used for patients with a history of allergy to the contrast substance, asthma, or serious renal disorder.

In T2*-WI, metallic implants such as seeds make the magnetic field inhomogeneous, and these inhomogeneities cause faster T2* relaxation resulting in loss of signal intensity and production of signal intensity artifacts;[12] therefore, it is easy to detect seeds. Prostate and urethra are poorly defined in T2*-WI and well defined in T2-WI,[20] so we used T2*-WI/T2-WI fusion for postimplant dosimetry. The

approximate time required for T2*-WI/T2-WI fusion-based dosimetry was 20 to 30 min, the same as that required for CT/T2-WI fusion-based dosimetry. No intravenous contrast material is required for the acquisition of T2*-WI.

All the DVH parameters estimated by T2*-WI/T2-WI fusion-based dosimetry strongly correlated to those estimated by CT/T2-WI fusion-based dosimetry in our results ($0.77 \leq R \leq 0.91$). Except for prostate V150 (95% CI, 0.08–3.19; $p = 0.04$), no significant difference was observed in these parameters between the two methods. These results show that T2*-WI/T2-WI fusion-based dosimetry is comparable to MRI-based dosimetry, as has been previously reported.

For some patients, large differences were observed in the values between the two methods. We thought these large differences resulted from seed miscounts in T2*-WI and shifts in fusion. The miscounts mainly occurred in clusters of seeds. It is difficult to correctly count the number of clustered seeds in T2*-WI because clustered seeds produce a large signal void. The finding that the prostate V150 value estimated by T2*-WI/T2-WI fusion-based dosimetry was significantly lower than that estimated by CT/T2-WI fusion-based dosimetry might also be due to underestimation of the number of clustered seeds in T2*-WI. This is because there is a high-dose area, like 150% of the prescribed dose, spread around the clustered seeds. We thought the primary cause of the shifts in T2*-WI/T2-WI fusion was prostate movement while T2*-WI and T2-WI were obtained.

Higher magnetic field strengths such as 3 tesla (T) and a higher-performance coil may improve the image quality of T2*-WI and the image acquisition speed of T2*-WI and T2-WI.[21,22] Thus, in the future, seed miscounts and fusion shifts may decrease, and T2*-WI/T2-WI fusion may be more useful for postimplant dosimetry of prostate brachytherapy.

REFERENCES

1. Blasko JC, *et al* (2002) Brachytherapy for carcinoma of the prostate: techniques, patient selection, and clinical outcomes. Semin Radiat Oncol **12**: 81–94.
2. Battermann JJ, Boon TA and Moerland MA (2004) Results of permanent prostate brachytherapy, 13 years of experience at a single institution. Radiother Oncol **71**: 23–28.
3. Nag S, *et al* (2000) The American Brachytherapy Society recommendations for permanent prostate brachytherapy postimplant dosimetric analysis. Int J Radiat Oncol Biol Phys **46**: 221–230.
4. Ash D, *et al* (2000) ESTRO/EAU/EORTC recommendations on permanent seed implantation for localized prostate cancer. Radiother Oncol **57**: 315–321.
5. Stone NN, *et al* (2007) Customized dose prescription for permanent prostate brachytherapy: insights from a multicenter analysis of dosimetry outcomes. Int J Radiat Oncol Biol Phys **69**: 1472–1477.
6. Zelefsky MJ, *et al* (2007) Intraoperative real-time planned conformal prostate brachytherapy: post-implantation dosimetric outcome and clinical implications. Radiother Oncol **84**: 185–189.
7. McElveen TL, *et al* (2005) Factors predicting for urinary incontinence following prostate brachytherapy. In: Dicker AP, Merrick GS, Waterman FM, Valicenti RK and Gomella LG eds. Basic and Advanced Techniques in Prostate Brachytherapy. pp. 441–451, Taylor & Francis; Abingdon.
8. Waterman FM and Dicker AP (2003) Probability of late rectal morbidity in 125I prostate brachytherapy. Int J Radiat Oncol Biol Phys **55**: 342–353.
9. Aoki M, Yorozu A and Dokiya T (2009) Results of a dummy run of postimplant dosimetry between multi-institutional centers in prostate brachytherapy with 125I seeds. Jpn J Radiol **27**: 410–415.
10. Tanaka O, *et al* (2006) Comparison of MRI-based and CT/MRI fusion-based postimplant dosimetric analysis of prostate brachytherapy. Int J Radiat Oncol Biol Phys **66**: 597–602.
11. Moerland MA, *et al* (2009) Decline of dose coverage between intraoperative planning and post implant dosimetry for I-125 permanent prostate brachytherapy: comparison between loose and stranded seed implants. Radiother Oncol **91**: 202–206.
12. Chavhan GB, *et al* (2009) Principles, techniques, and applications of T2*-based MR imaging and its special applications. Radiographics **29**: 1433–1449.
13. Rivard MJ, *et al* (2004) Update of AAPM Task Group No. 43 Report: A revised AAPM protocol for brachytherapy dose calculations. Med Phys **31**: 633–674.
14. Crook J, *et al* (2002) Interobserver variation in postimplant computed tomography contouring affects quality assessment of prostate brachytherapy. Brachytherapy **1**: 66–73.
15. Stone NN, *et al* (2003) Comparison of intraoperative dosimetric implant representation with postimplant dosimetry in patients receiving prostate brachytherapy. Brachytherapy **2**: 17–25.
16. Vidakovic S, *et al* (2007) Post-implant computed tomography-magnetic resonance prostate image registration using feature line parallelization and normalized mutual information. J Appl Clin Med Phys **8**: 21–32.
17. Amdur RJ, *et al* (1999) Prostate seed implant quality assessment using MR and CT image fusion. Int J Radiat Oncol Biol Phys **43**: 67–72.
18. Polo A, *et al* (2004) MR and CT image fusion for postimplant analysis in permanent prostate seed implants. Int J Radiat Oncol Biol Phys **60**: 1572–1579.
19. Tanaka O, *et al* (2006) Importance of the CT/MRI fusion method as a learning tool for CT-based postimplant dosimetry in prostate brachytherapy. Radiother Oncol **81**: 303–308.
20. Chernoff DM and Hricak H (1997) The male pelvis: prostate and seminal vesicles. In: Higgins CB, Hricak H and Helms CA eds. Magnetic Resonance Imaging of the Body. 3rd ed. pp. 875–900, Lippincott-Raven Publishers; Philadelphia.
21. Takahashi M, Uematsu H and Hatabu H (2003) MR imaging at high magnetic fields. Eur J Radiol **46**: 45–52.
22. Reiser M and Faber SC (1997) Recent and future advances in high-speed imaging. Eur Radiol **7**(Suppl 5): 166–173.

Received on January 28, 2011
Revision received on June 3, 2011
Accepted on June 29, 2011
J-STAGE Advance Publication Date: August 20, 2011